Supplementary Information for

Cryo-EM structure of the *Agrobacterium tumefaciens* type IV secretion system-associated T-pilus reveals stoichiometric protein-phospholipid assembly

Stefan Kreida[1#], Akihiro Narita[2#], Matthew D Johnson[3], Elitza I Tocheva[4], Anath Das[5], Debnath Ghosal[3,6,*], Grant J. Jensen[1,7,*]

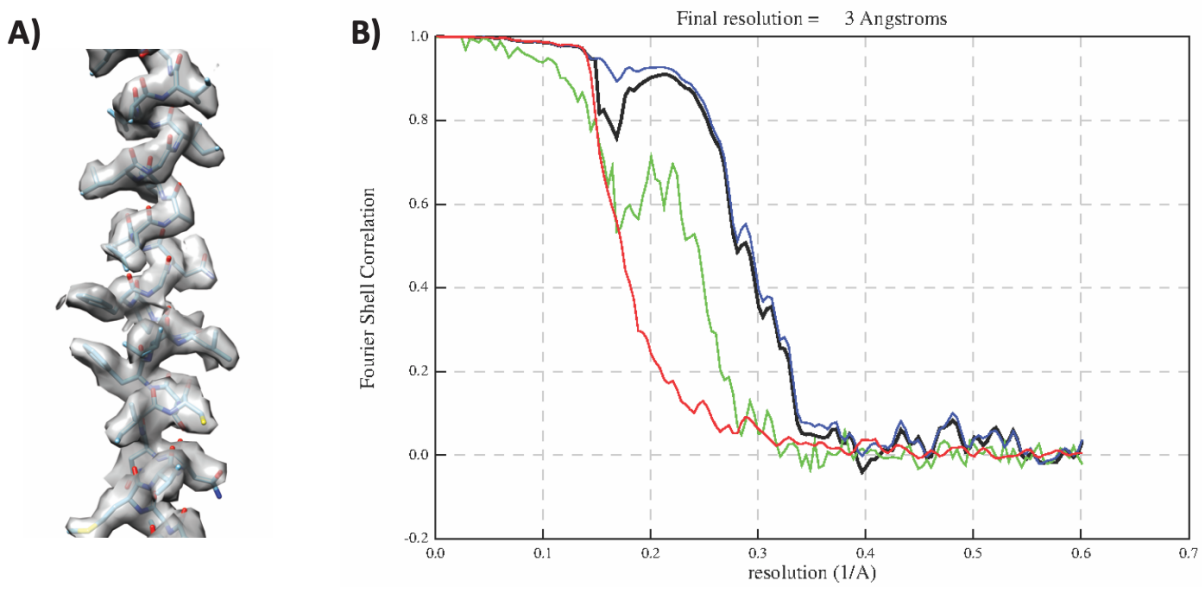

Figure S1. Resolution estimation, related to STAR Methods. (A) Representative region of VirB2 monomer showing the fit of the atomic model to the experimentally derived cryo-EM density map. (B) Fourier shell correlations (FSCs) for evaluating the resolution calculated by RELION.[33] FSCs between two 3D structures from each half of the dataset with or without masking are presented in green and blue, respectively. The red curve was calculated after the phase was randomized beyond 6.9 Å to evaluate the artifacts from overfitting. The black curve is the corrected FSC after accounting for the artifacts from overfitting. Based on the gold-standard criteria between two half-maps, the resolution is 3.0 Å with a threshold of 0.143.

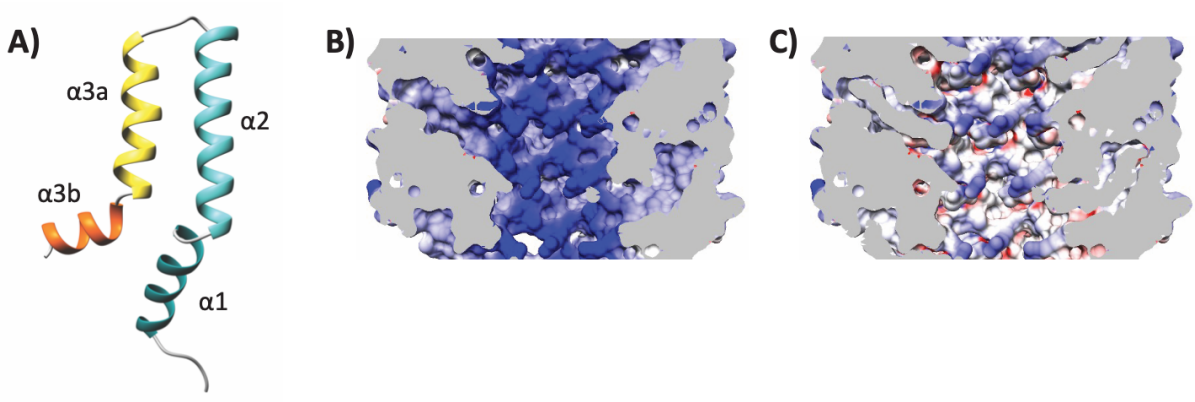

Figure S2. VirB2 monomer and luminal electrostatic potential, related to Figure 4. (A) VirB2 monomer showing 4 helices (α1, α2, α3a and α3b). (B-C) Electrostatic potential of the T-pilus lumen shown (B) without lipid and (C) with lipid. Electrostatic potential of the lumen was calculated using Chimera.

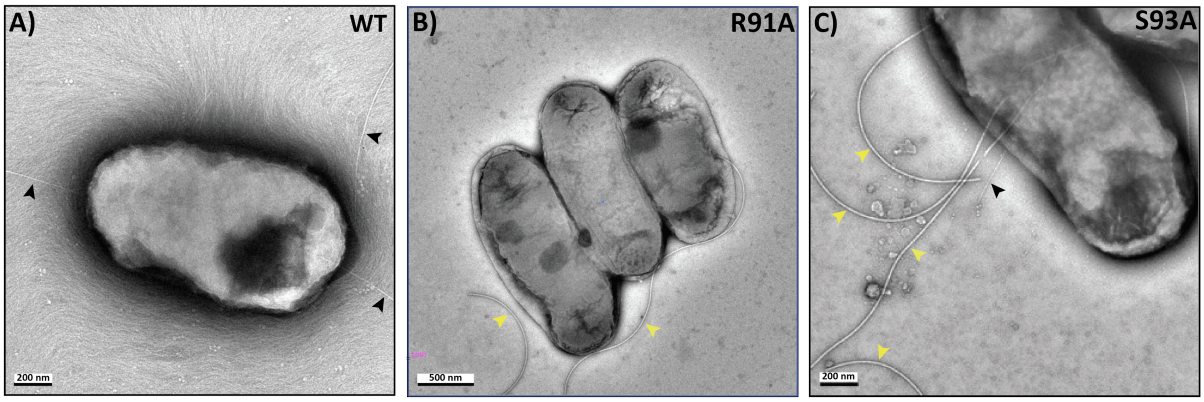

Figure S3. Effect of R91 mutation on T-pilus formation, related to Figure 5. Negatively stained micrographs of (A) WT, (B) R91A and (C) S93A mutants showing presence of T-pili (WT and S93A) and absence (R91A) of T-pilus, respectively. Black arrows show T-pili (~10 nm in diameter), yellow arrows show flagella. Scale bar, as shown on the micrographs. The swirl-like pattern in A is a staining gradient of the formvar surface spreading from the height of the cell.

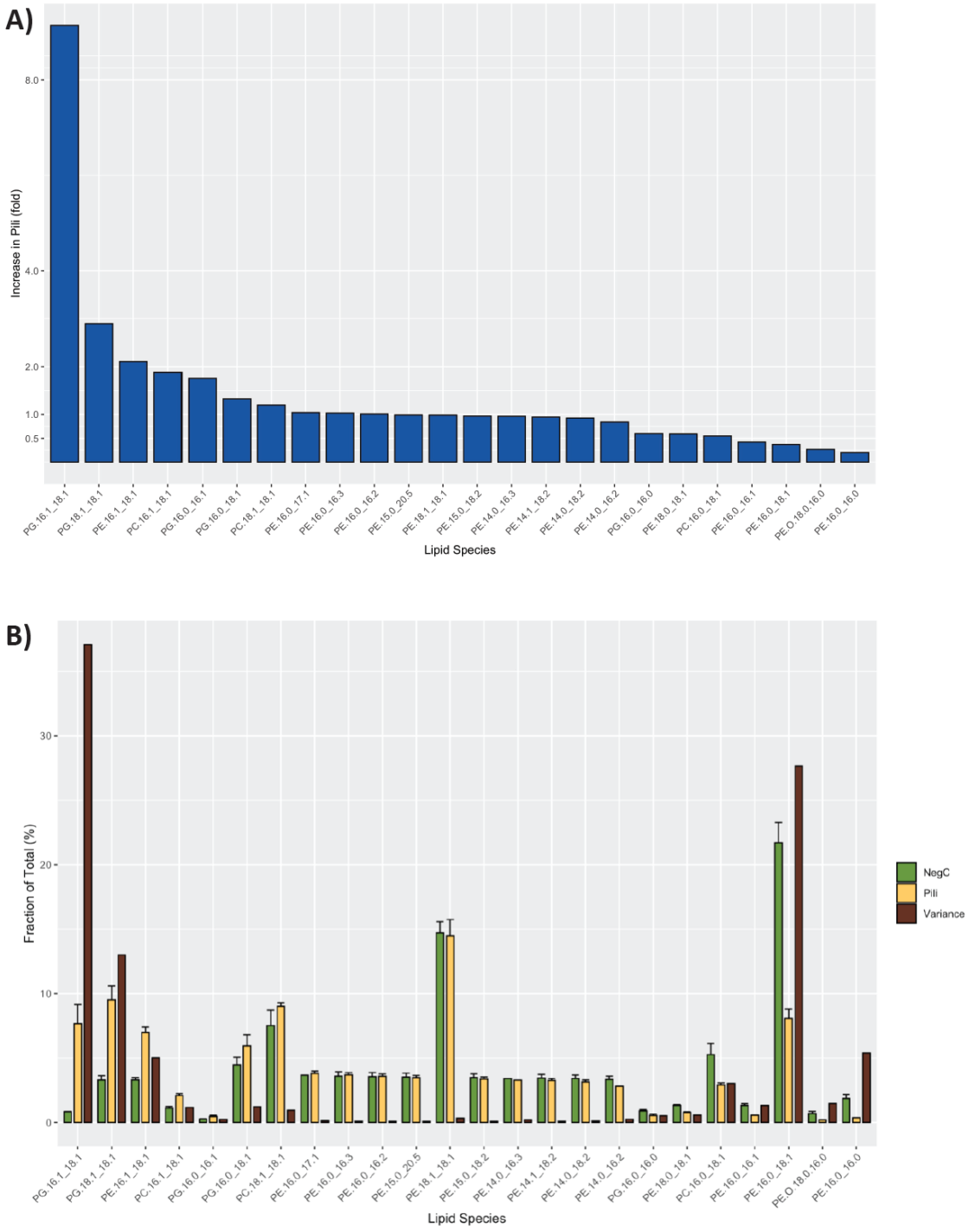

Figure S4. Lipidomic analysis of the T-pilus, related to Figure 2. (A) Barplot showing the fold increase of each analyzed lipid species in the pili-containing sample compared to the negative control (B) Barplot showing relative abundances of lipid species (in percent) in purified pilus sample (yellow) and negative control (green), as an average of three independent experiments. The bars are ordered by the fold increase in pili. Error bars show the standard deviation for triplicates. The variance was

calculated for each lipid species for all six observations (three from pilus, and three from negative control) on CLR-transformed data. This value was then divided by the summed variance of all species. This Contribution to Total Variance (in percent) for each lipid species is shown in brown.

Table S1. Cryo-EM data collection, refinement and validation, related to STAR Methods.

Table S1. Cryo-EM data collection, refinement and validation statistics	
Parameter	
Data collection and processing	
Voltage (kV)	300
Electron exposure (e–/Å2)	60
Pixel size (Å)	0.832
Final particle images (n)	3543
Helical symmetry	
Point group	C5
Helical rise (Å)	13.4
Helical twist (°)	32.6
Map resolution (Å)	
Map:map FSC (0.143)	3.0
Model:map FSC (0.143)	2.5
D_{99}	2.6
Refinement and model validation	
B-factor (Å2)	-75.4
Bond length RMSD (Å)	0.004
Bond angles RMSD (°)	0.818
Model:map RSCC	0.8
Clash score	3.2
Poor rotamer (%)	0
Ramachandran favoured	100
Ramachandran outlier	0
Molprobity score	1.11
Deposition ID	
PDB (model)	8FAI
EMDB (map)	EMD-28957

Table S2. Lipidomic analysis of the T-pilus, related to STAR Methods. Relative abundances of lipid species with SD in pili-containing samples and negative control as an average of three independent preparations.

Lipid Species	Pili (%)	NegC (%)	Increase in Pili (fold)	Contribution to Total Variance (%)
PG.16.1_18.1	**7.67** ± 1.48	**0.84** ± 0.01	**9.14**	**37.06**
PG.18.1_18.1	**9.52** ± 1.06	**3.29** ± 0.33	**2.89**	**13.00**
PE.16.1_18.1	**6.97** ± 0.43	**3.30** ± 0.19	**2.11**	**5.01**
PC.16.1_18.1	**2.09** ± 0.14	**1.11** ± 0.13	**1.88**	**1.16**
PG.16.0_16.1	**0.46** ± 0.09	**0.26** ± 0.02	**1.76**	**0.24**
PG.16.0_18.1	**5.94** ± 0.87	**4.47** ± 0.58	**1.33**	**1.22**
PC.18.1_18.1	**9.02** ± 0.24	**7.52** ± 1.19	**1.20**	**0.94**
PE.16.0_17.1	**3.80** ± 0.19	**3.67**	**1.04**	**0.12**
PE.16.0_16.3	**3.69** ± 0.18	**3.59** ± 0.34	**1.03**	**0.09**
PE.16.0_16.2	**3.59** ± 0.18	**3.56** ± 0.32	**1.01**	**0.08**
PE.18.1_18.1	**14.49** ± 1.26	**14.70** ± 0.87	**0.99**	**0.34**
PE.15.0_20.5	**3.48** ± 0.17	**3.52** ± 0.31	**0.99**	**0.07**
PE.15.0_18.2	**3.37** ± 0.16	**3.49** ± 0.29	**0.97**	**0.08**
PE.14.0_16.3	**3.28**	**3.41**	**0.96**	**0.19**
PE.14.1_18.2	**3.26** ± 0.16	**3.45** ± 0.28	**0.94**	**0.09**
PE.14.0_18.2	**3.15** ± 0.15	**3.41** ± 0.27	**0.92**	**0.11**
PE.14.0_16.2	**2.81**	**3.34** ± 0.26	**0.84**	**0.25**
PG.16.0_16.0	**0.54** ± 0.12	**0.89** ± 0.10	**0.60**	**0.52**
PE.18.0_18.1	**0.78** ± 0.04	**1.32** ± 0.06	**0.59**	**0.57**
PC.16.0_18.1	**2.90** ± 0.17	**5.26** ± 0.85	**0.55**	**3.03**
PE.16.0_16.1	**0.56** ± 0.01	**1.32** ± 0.13	**0.42**	**1.32**
PE.16.0_18.1	**8.08** ± 0.70	**21.71** ± 1.56	**0.37**	**27.67**
PE.O.18.0.16.0	**0.19** ± 0.01	**0.70** ± 0.17	**0.27**	**1.46**
PE.16.0_16.0	**0.37** ± 0.01	**1.86** ± 0.31	**0.20**	**5.39**